ELSEVIER

Journal of Molecular Structure: THEOCHEM 758 (2006) 53–60

THEO CHEM

www.elsevier.com/locate/theochem

Kinetic study of the hydrogen abstraction reaction $H_2O_2 + H \rightarrow H_2 + HO_2$ by ab initio and density functional theory calculations

Y. Tarchouna, M. Bahri *, N. Jaïdane, Z. Ben Lakhdar

Laboratoire de Spectroscopie Atomique Moléculaire et Applications, Département de Physique, Faculté des Sciences, Université Tunis-El Manar, le Belvédère 1060 Tunis, Tunisie

Received 17 February 2005; received in revised form 29 September 2005; accepted 7 October 2005

Abstract

A theoretical kinetic study of the elementary chemical reaction involving hydrogen atom abstraction from hydrogen peroxide by hydrogen atom leading to H_2 molecule and HO_2 radical was reported. Rate constants were calculated using transition state theory. The values of the kinetic parameters, the classical barrier height and the pre-exponential factor, were derived from ab initio (MP2//CASSCF) and density functional theory calculations of the electronic structure of each chemical species implied in the title reaction using the aug-cc-pVTZ basis set. Two hybrid BHHLYP and B3LYP functionals were used. The ZPE and BSSE corrected classical barrier height was predicted to be 9.31 and 2.34 kcal mol^{-1}, respectively, for the two used DFT methods and 8.08 kcal mol^{-1} for the ab initio calculation. The experimental value derived from fitted Arrhenius expressions ranges from 3.75 to 9.44 kcal mol^{-1}. The rate constants based on the ab initio and on the BHHLYP calculations were found to be in reasonable agreement with the available observed ones. However, those based on the B3LYP calculation were found to be far from accurately predicted.

Keywords: Hydrogen peroxide; Hydrogen atom; Ab initio; DFT; TST

1. Introduction

Elementary reactions involving the hydrogen atom transfer from a stable molecule to an atom or radical, commonly called hydrogen abstraction reactions, have received considerable attention in the literature due to their importance in both combustion and atmospheric chemistry. Most of the theoretical studies performed on these kinds of reactions were interested in those involving a primary, secondary or tertiary hydrogen atom abstraction from saturated, unsaturated, halogen-substituted, oxygenated and polycyclic aromatic hydrocarbons [1–10]. All these reactions were considered to take place via a C–H bond breaking path. Thermal rate constants $k(T)$ calculated using transition state theory (TST) depend strongly on the kinetic parameters both the activation barrier and the pre-exponential factor. Several methods based on the density functional theory (DFT) were tested in reproducing accurate kinetic parameters and rate constants for this kind of hydrogen abstraction reactions [11–14]. However, there are a few studies on the hydrogen abstraction reaction involving O–H bond breaking [15–17]. In previous published works [18–20], ab-initio-TST method was used to study hydrogen abstraction from the hydrogen peroxide H_2O_2 molecule by H, O atoms and OH radical:

$$H_2O_2 + H \rightarrow H_2 + HO_2 \quad (1)$$

$$H_2O_2 + O(^3P) \rightarrow OH + HO_2 \quad (2)$$

$$H_2O_2 + OH \rightarrow H_2O + HO_2 \quad (3)$$

Recently, R.G. Susnow et al. [21] indicated that they have attempted to study H abstraction from hydrogen peroxide by DFT-TST method but they found that the predicted rate constants were grossly in error. Therefore, they did not show their results.

To our knowledge, DFT-TST rate constants of reactions (1)–(3) are not available.

In this paper, we will report (ab initio)-TST and DFT-TST kinetic study of reaction (1). Two hybrid functionals namely BHHLYP and B3LYP will be used to calculate the electronic structures of the reactants, the products and the activated

* Corresponding author. Present address: Département de physique Faculté des Sciences B.P.802, Sfax 3018, Tunisie. Tel.: +216 4276400; fax: +216 4274437.

E-mail address: mohamed.bahri@fss.rnu.tn (M. Bahri).

0166-1280/$ - see front matter © 2006 Elsevier B.V. All rights reserved.
doi:10.1016/j.theochem.2005.10.003

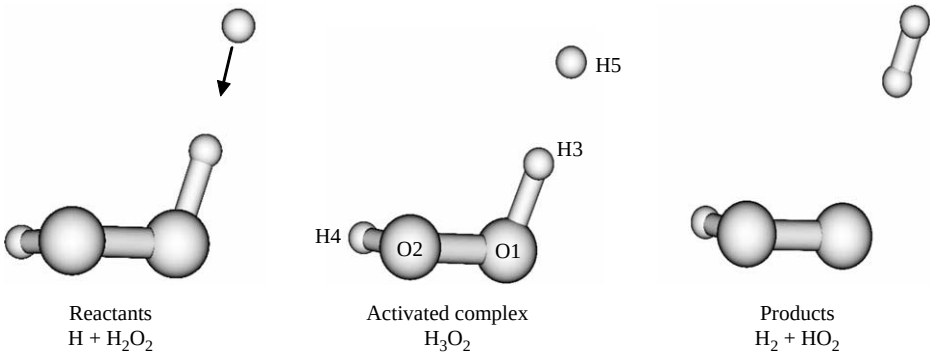

FIG. 1. Assumed mechanism for H_2O_2+H hydrogen abstraction reaction.

complex involved in reaction (1). The electronic structure results will be used together with the TST method to evaluate the thermal rate constants over the range of temperature $200 \leq T \leq 2000$ K. The experimental preferred values of $k(T)$ for reaction (1) are those measured by Baulch et al. [22] and Warnatz [23], which are fitted by the same Arrhenius expression $k(T)=2.8\ 10^{-12}\exp(-1890\ \mathrm{K/T})\ \mathrm{cm^3\ mol^{-1}\ s^{-1}}$ for $300 \leq T \leq 800$ K. The measured ones by Stang and Hampson [24] are fitted by the expression $k(T)=8.0\ 10^{-11}\exp(-4005\ \mathrm{K/T})\ \mathrm{cm^3\ mol^{-1}\ s^{-1}}$ for $300 \leq T \leq 2500$ K. Finally, the reliability of the theoretical DFT-TST method in predicting kinetics of hydrogen abstraction reactions involving O–H bond breaking by H atom will be discussed.

2. Computational method

2.1. Electronic structure calculation

The minimum energy structure, the harmonic vibrational frequencies and the zero point energy (ZPE) corrections for the reactants, products and the transition state (H_3O_2) complex involved in the title reaction were calculated using one ab initio and two DFT methods. All calculations were performed with the GAMESS program [25] using the aug-cc-pVTZ basis set [26]. Reaction (1) was assumed to take place via the hydrogen abstraction path, where a hydrogen atom moves from the H_2O_2 molecule to the H atom leading to the H_2 molecule and HO_2 radical as shown in Fig. 1. No symmetry constraint was used for all species implied in reaction (1). Each species was taken to be in the ground state. The basis set superposition error (BSSE) was calculated for the transition state according to the Boys–Bernardi counterpoise scheme [27].

2.1.1. DFT calculation

Two exchange/correlation BHHLYP (50% HF plus 50% B88 exchange with LYP correlation) and B3LYP methods were used. For open shell systems (H_3O_2 and HO_2) both the BHHLYP and the B3LYP calculations were based on the ROHF wave function of the doublet state.

2.1.2. Ab initio calculation

The ab initio calculations were performed at the CASSCF level using, for each molecular species, the same active space as described in our previous work [18]. Using the CASSCF wave function at the optimum geometry of each species, the energy was corrected for the remaining electron correlation in a second order perturbation MP2 calculation with the MCQDPT2 method of Nakano [28,29]. All inactive electrons (not correlated at the CASSCF method) were included in the MP2 calculation.

2.2. Rate constant calculation

Rate constants are calculated, as a function of temperature T, in the zero order semi-classical interpolated transition state theory [30]. In this model information needed is only available at the reactant (R), the saddle point ($\neq$) and product (P) and the rate constant is given by:

$$k(T) = \kappa(T) \times k_{\mathrm{TST}}(T), \tag{4}$$

where

$$k_{\mathrm{TST}}(T) = \frac{\sigma}{\beta h} \times \frac{Q^{\neq}(T)}{Q^{R}(T)} \times e^{-\beta V^{\neq}} \tag{5}$$

is the conventional transition state theory (TST) rate constant without tunneling correction. $\sigma=2$ (for this reaction) are the symmetry factor accounting for the two possibilities of hydrogen abstraction reaction from H_2O_2. $\beta=(1)/(K_BT)$, K_B is Boltzmann's constant, h is Plank's constant, $Q^{R}(T)$ and $Q^{\neq}(T)$ are, respectively, the reactant and the transition state partition functions per unit of volume and $V^{\neq}$ is the classical barrier height. To evaluate $Q^{R}(T)$, $Q^{\neq}(T)$ and $V^{\neq}$ we need the geometry, the energy and the vibrational frequencies of reactants and activated complex. These quantities are provided by the ab initio and the DFT calculations.

$\kappa(T)$ is a ground state transmission coefficient, which primarily accounts for tunneling correction. In this work, we have evaluated this coefficient with two different methods: the Wigner (W) [31] and the zero curvature tunneling (ZCT) [32] methods. The Wigner transmission coefficient is given by the formula:

$$\kappa(T) = 1 + \frac{1}{24}\left|\frac{\hbar\omega^{\neq}}{K_B T}\right|^2 \tag{6}$$

$\omega^{\neq}$ is the imaginary frequency of the transition state.

For details about the ZCT transmission coefficient see indicated reference.

The two tunneling corrected rate constants are noted, respectively, by $k_{TST/W}$ and $k_{TST/ZCT}$.

All the rate constant calculations were done with the POLYRATE 8.0 program [33].

3. Results and discussion

3.1. Electronic structure calculation

This section presents the result of the MP2//CASSCF and the DFT calculations relative to the minimum energy structure, the harmonic vibrational frequencies and the energy of each species implied in reaction (1). As rotational and vibrational partition function of the reactants and the activated complex, which serve to evaluate the TST rate constant, depend, respectively, on the optimized structures and the vibrational frequencies. The reliability of the ab initio and the DFT calculation was tested by comparing our results with the available experimental ones.

3.1.1. Minimum energy structure

The optimized geometry parameters for the minimum energy structure of all species involved in reaction (1) are reported and compared to available experimental ones in Table 1. Inspection of this table shows that the calculated bond lengths in H_2, H_2O_2 and HO_2 agree with the experimental data within 2.9% for CASSCF, 3.5% for BHHLYP and 0.8% for B3LYP methods. Bending and dihedral angles are predicted with an error never exceeding 3.6% for CASSCF, 2.5% for BHHLYP and 1.3% for B3LYP calculations. This agreement between calculated and experimental structures ensures that the resulting moments of inertia of all species are predicted with a reasonable accuracy.

No experimental structures of transition states are available, however our calculation results relative to the optimisation of the activated complex (H_3O_2) showed a reasonable structure. The geometrical parameters R(O1–O2), R(O2–H4) and θ(O1O2H4) related to the non-reactive moiety in H_3O_2 took intermediate values between their homologues in H_2O_2 (reactant) and in HO_2 (product). The dihedral angle α(H3O1O2H4) of H4 in H_3O_2 was smaller than that in H_2O_2 by about 17% for the CASSCF and 14% for the two DFT calculations. Inspection of the results relative to the geometrical parameters R(O1– H3) and R(H3–H5) of the reactive moiety in H_3O_2 showed that, for reaction (1) to take place via the H abstraction path, the broken R(O1– H3) bond must be stretched by about 25% for CASSCF, 18% for BHHLYP and 13% for B3LYP. The formed R(H3–H5) bond must have a value far from that in H_2 by, respectively, 25, 30 and 41%. These described changes in the broken and formed bonds showed that the CASSCF and the two DFT methods provide a reactant-like character for the transition state which is consistent with the exothermic character of the reaction. The bending angle θ(O1H3H5) was predicted to be close to 180° for the three methods; namely for CASSCF 176.3°, for BHHLYP 176.2° and for B3LYP 175.5°. This indicates that the preferred bringing together of H atom and H_2O_2 molecule to react via H abstraction path is the one where O1, H3 and H5 atoms are near linear. This has already been observed in other H abstraction reactions [19,20,36–38]. Fig. 2 shows the BHHLYP, the B3LYP and the CASSCF iso-density curve relative to the $\sigma_{O_1-H_3}$ orbital in the H_3O_2 complex. It can be noted that the probability to find the electrons occupying the $\sigma_{O_1-H_3}$ orbital in the region between H3 and H5 atoms is important. So the O1–H3 bond at the TS is ready to be broken while the H3–H5 bond at the TS is ready to be formed. This is consistent with the hydrogen abstraction reaction hypothesis and indicates that, for each used method, the adequate TS structure was located.

Table 1
Calculated geometrical parameters of H_2, HO_2, H_2O_2 and H_3O_2 (Bond length in Å, angles in degrees)

System	Parameters[a,b]	CASSCF	BHHLYP	B3LYP	Exp[c]
H_2	R(H–H)	0.750	0.737	0.743	0.741
HO_2	R(O–O)	1.374	1.304	1.327	1.335
	R(O–H)	0.969	0.961	0.976	0.977
	θ(OOH)	102.8	106.0	105.5	104.1
H_2O_2	R(O–O)	1.475	1.413	1.451	1.464
	R(O–H)	0.967	0.954	0.967	0.965
	θ(O–O–H)	99.3	101.9	100.7	99.4
	α(H–O–O–H)	115.9	112.5	113.3	111.8
H_2O_3	R(O–O)	1.445	1.370	1.407	
	R(O1–H3)	1.214	1.127	1.095	
	R(O2–H4)	0.968	0.956	0.969	
	R(H3–H5)	0.937	0.959	1.048	
	θ(O2O1H3)	101.8	106.0	105.6	
	θ(O1H3H5)	176.3	176.2	175.5	
	θ(O1O2H4)	100.6	103.8	102.6	
	α(H4O2O1H3)	96.5	96.7	98.8	
	α(H5H3O1O2)	−26.3	−66.7	−112.5	

[a] See Fig. 1.
[b] R, stretch; θ, bending angle; α, tortional angle.
[c] Ref. [34] for H_2 and [35] for HO_2 and H_2O_2.

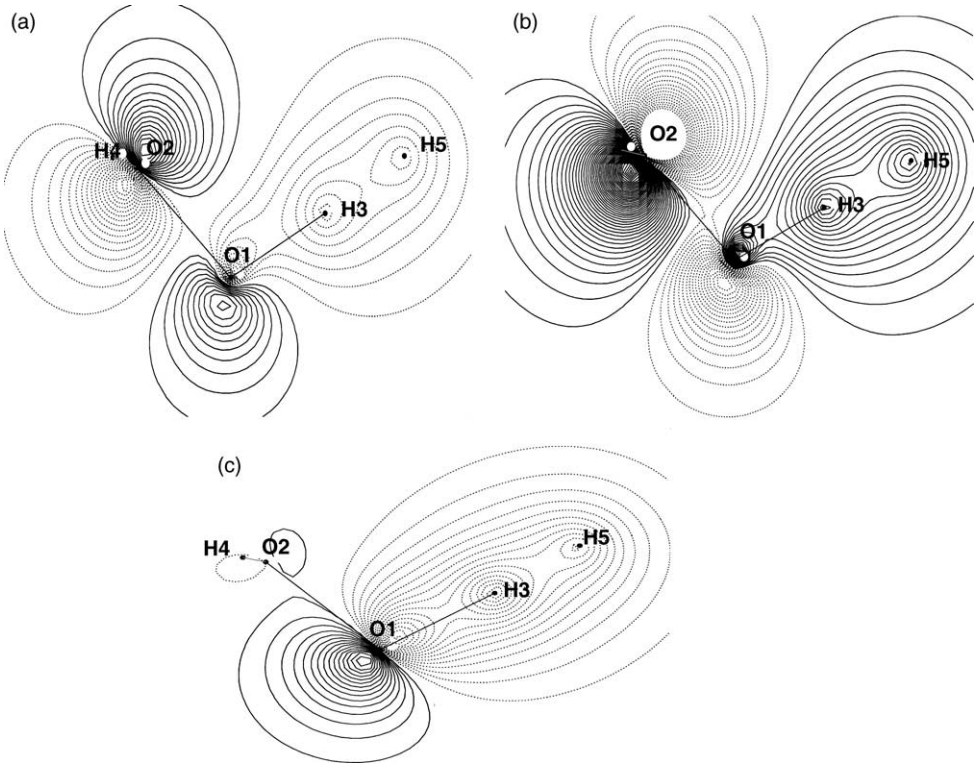

Fig. 2. Isodensity curves corresponding to the σ(O1–H3) orbital in H_3O_2: (a) BHHLYP, (b) B3LYP, and (c) CASSCF calculations.

3.1.2. Vibrational frequencies

The calculated CASSCF, BHHLYP and B3LYP harmonic vibrational frequencies for the equilibrium structures of HO_2, H_2, H_2O_2 and H_3O_2 are listed and compared to available experimental ones in Table 2. We note that the CASSCF calculation reproduce the observed frequencies with un error never exceeds 8% for stretching mode and 16.7% for the other modes. The disagreement between the BHHLYP and the experimental frequencies lay between 2.6 and 11.0% for the stretching mode and 6.1 and 19.9% for the other modes. The calculated B3LYP frequencies agreed well with the experimental values. This agreement could drop below 0.5% and did not exceed 5% for the stretching modes and 7.5% for the other modes. The Hessian matrix of the transition state possesses only one imaginary frequency $\omega^{\neq}$. To ensure that the right transition state was located, the imaginary normal mode was decomposed into the nine internal coordinates by the method of Boatz and Gordon [44], the result is given in Table 3. This table seems to show clearly that, for each used method, the major contribution to this mode come from the

Table 2
Harmonic vibrational frequencies (cm^{-1}) of the equilibrium structure for H_2, HO_2, H_2O_2 and H_3O_2

System	CASSCF	BHHLYP	B3LYP	Exp[a]
H_2	4299.3(2.3)	4517.1 (2.6)*	4414.3 (0.3)	4401.2
HO_2	913.6(16.7)	1243.8 (13.3)	1158.4 (5.5)	1097.6
	1486.1(6.8)	1513.7 (8.7)	1430.3 (2.8)	1391.8
	3710.1(7.9)	3816.1 (11.0)	3587.5 (4.4)	3436.2
H_2O_2	348.4(6.1)	394.0 (6.1)	373.1 (0.6)	371[b]
	840.3(4.3)	1053.0 (19.9)	944.1 (7.5)	878[c]
	1339.1(5.1)	1388.5 (8.9)	1308.8 (2.7)	1274[d]
	1451.9(4.1)	1505.2 (8.0)	1423.1 (2.1)	1394[e]
	3740.6(3.6)	3939.3 (9.1)	3753.0 (4.0)	3610[b]
	3742.6(3.4)	3940.3 (8.9)	3753.8 (3.7)	3619[b]
H_3O_2	374.4	425.7	398.3	
	395.1	463.5	430.6	
	788.4	766.5	720.1	
	836.3	1101.8	1008.9	
	1158.9	1325.2	1322.1	
	1423.2	1473.2	1385.4	
	1512.9	1602.9	1535.5	
	3717.3	3900.4	3711.1	
	2901.8 I	2744.5 I	1600.8 I	

Value in parenthesis represents the error (in %) of calculation with respect to experience.

[a] Ref. [34] for H_2 and [39] for HO_2.

[b] Ref. [40].

[c] Ref. [41].

[d] Ref. [42].

[e] Ref. [43].

Table 3
Decomposition of the imaginary normal mode into the nine internal coordinates

Internal coordinate	CASSCF	BHHLYP	B3LYP
R(O1–O2)	−0.0294	−0.0533	−0.0732
R(O1–H3)	0.9922	0.9669	0.8714
R(O2–H4)	0.0049	0.0113	0.0110
R(H3–H5)	−1.1876	−1.2265	−1.3156
θ(O2O1H3)	−0.0041	0.0168	0.0605
θ(O1O2H4)	0.0036	0.0106	0.0199
θ(O1H3H5)	−0.0454	−0.0371	0.0498
α(H4O2O1H3)	−0.0108	−0.0156	−0.0406
α(H5H3O1O2)	0.2224	0.7952	1.0872

Table 4
Total energies (a.u) of H_2, HO_2, H_2O_2 and H_3O_2 (the energy value of H atom is calculated at the ROHF level −0.4998338396 a.u)

System	MP2//CASSCF	BHHLYP	B3LYP
H_2	−1.1704545243(6.1)*	−1.1701513348 (6.5)	−1.1732913398 (6.3)
HO_2	−150.7389224460(8.7)	−150.8915337669 (9.4)	−150.9097790762 (8.8)
H_2O_2	−151.3883547201(16.4)	−151.5340614446 (17.5)	−151.5529230568 (16.5)
H_3O_2	−151.8737810845(14.6)	−152.0164340467 (15.8)	−152.0467407407 (15.0)

*Values in parenthesis are the ZPE in kcal mol^{-1}.

Table 5
Total energies (a.u.) used to evaluate the BSSE correction (kcal mol^{-1}) for the H_3O_2 complex

	MP2//CASSCF	BHHLYP	B3LYP
$E^{H3O2}(H_2O_2)$[a]	−151.3580224690	−151.5124319547	−151.5407921799
$E^{H2O2}(H_2O_2)$	−151.3566614348	−151.5123577194	−151.5406941917
$E^{H3O2}(H)$[b]	−0.4998395430	−0.4998399651	−0.4998393062
ΔBSSE	0.85	0.05	0.06

[a] $E^{H3O2}(H_2O_2)$ is the energy of the H_2O_2 moiety in the activated complex calculated using the basis set of H_3O_2.
[b] $E^{H3O2}(H)$ was calculated at the ROHF level using the geometry of the activated complex optimised at the correlated level(CASSCF or BHHLYP or B3LYP). For $E^{H}(H)$ we have used the same value as indicated in Table 4.

breaking stretch R(O1– H3), the formed one R(H3–H5) and the dihedral angle of the approached atom H5. This means that the reaction coordinate corresponds to the motion of the H3 atom between O1 and H5. Animation of the imaginary normal mode was done using the MOLDEN Package [45] to confirm that the adequate TS were located. The CASSCF, BHHLYP and B3LYP value of the magnitude ($\omega\neq$(of $\omega^{\neq}$ was found to be, respectively, 2901.8, 2744.5 and 1600.8 cm^{-1}. As ($\omega^{\neq}$(is related to the curvature of the potential energy surface (PES) near the TS, the B3LYP calculation provided a PES flatter than the one predicted by the CASSCF and the BHHLYP methods.

3.1.3. Energetics

The calculated MP2//CASSCF, BHHLYP and B3LYP values of the total energies and the harmonic ZPE for all species involved in reaction (1) are listed in Table 4. In Table 5, total energies used to evaluate the BSSE correction for H_3O_2 are collected. For both BHHLYP and B3LYP methods the BSSE correction was found to be about 0.05 kcal mol^{-1} and then has a nearly negligible effect on the barrier height values. For the MP2//CASSCF calculation the BSSE is found to be 0.85 kcal mol^{-1}. Using Tables 4 and 5, the reaction energy E_r and the barrier height $V^{\neq}$ were calculated. The resulting values were collected and compared to the experimental ones in Table 6. This table indicates that, as it was well established for hydrogen abstraction reactions [1,14], the B3LYP computed barrier was too low. The BHHLYP method compared to the B3LYP one yielded more accurate reaction and activation energies for reaction (1). The ZPE corrected value of the reaction energy E_r overestimated the experimental one by about 2 kcal mol^{-1} for BHHLYP and 3 kcal mol^{-1} for B3LYP calculations. The MP2//CASSCF value of E_r underestimate the observed one by 2 kcal mol^{-1}. The BSSE and ZPE corrected BHHLYP barrier height is predicted to be 9.31 kcal mol^{-1} which differ from the correspondent MP2//CASSCF value by only 1.23 kcal mol^{-1} and lay in the range of experimental values fitted from Arrhenius expressions of the rate constants as a function of temperature.

However, it is necessary to notice that in some works in preparation B3LYP method was found to predict accurate reaction and activation energies for a non-hydrogen abstraction path of H_2O_2+H reaction [47]. The calculated values were found to be −68.22 kcal mol^{-1} for the reaction energy and 3.96 kcal mol^{-1} for the barrier height. The experimental ones were, respectively, −68.18 and 3.57 kcal mol^{-1} [22].

3.2. Rate constant calculation

Although the ability of the B3LYP method to predict accurate structures and vibrational frequencies of reactants and

Table 6
Reaction energy E_r and barrier height $V^{\neq}$ in kcal mol^{-1} for reaction (1)

	MP2//CASSCF	BHHLYP	B3LYP	Exp.
E_r	−13.29(−15.09)*	−17.44(−19.04)	−19.02(−20.40)	−17.05[a]
$V^{\neq}$	9.04(8.08)	10.96(9.31)	3.77(2.34)	3.75 − 9.50[b]

*Values in parenthesis are the BSSE and/or ZPE corrected ones.
[a] Ref. [22].
[b] Refs. [22,46]

Table 7
Calculated BHHLYP-TST rate constants ($cm^3\ mol^{-1}\ s^{-1}$) compared to experimental values

$T(K)$	k_{TST}	$k_{TST/W}$	$k_{TST/ZCT}$	Exp.[a]	DF
200	2.34(−21)*	4.04(−20)	1.12(−15)		
250	2.34(−19)	2.67(−18)	1.79(−15)		
298	4.59(−18)	3.82(−17)	2.90(−15)	4.92(−15)	1.69
300	5.10(−18)	4.19(−17)	2.96(−15)	5.14(−15)	1.74
350	4.65(−17)	2.93(−16)	5.05(−15)	12.6(−15)	2.49
400	2.48(−16)	1.25(−15)	8.66(−15)	24.8(−15)	2.86
450	9.21(−16)	3.88(−15)	1.47(−14)	4.19(−14)	2.85
500	2.67(−15)	9.59(−15)	2.43(−14)	6.39(−14)	2.62
550	6.43(−15)	2.03(−14)	3.90(−14)	9.01(−14)	2.31
600	1.35(−14)	3.80(−14)	6.04(−14)	11.9(−14)	1.97
650	2.57(−14)	6.52(−14)	9.06(−14)	15.2(−14)	1.67
700	4.48(−14)	1.04(−13)	1.32(−13)	1.88(−13)	1.42
750	7.32(−14)	1.58(−13)	1.86(−13)	2.25(−13)	1.21
800	1.13(−13)	2.28(−13)	2.56(−13)	2.63(−13)	1.03
850	1.68(−13)	3.19(−13)	3.43(−13)	7.19(−13)	2.09
900	2.39(−13)	4.31(−13)	4.51(−13)	9.34(−13)	2.07
950	3.30(−13)	5.68(−13)	5.83(−13)	11.8(−13)	1.92
1000	4.43(−13)	7.31(−13)	7.39(−13)	14.5(−13)	1.96
1050	5.82(−13)	9.25(−13)	9.24(−13)	17.6(−13)	1.90
1100	7.48(−13)	1.15(−12)	1.14(−12)	2.09(−12)	1.83
1200	1.17(−12)	1.70(−12)	1.67(−12)	2.84(−12)	1.70
1300	1.74(−12)	2.41(−12)	2.35(−12)	3.67(−12)	1.56
1400	2.47(−12)	3.28(−12)	3.19(−12)	4.57(−12)	1.43
1500	3.37(−12)	4.34(−12)	4.21(−12)	5.54(−12)	1.32
2000	1.09(−11)	1.27(−11)	1.24(−11)	1.07(−11)	1.16

*Powers of ten are in parenthesis.
[a] Ref. [22] for $T \leq 800$ K and Ref. [23] for $800 < T \leq 2000$ K.

products, it has a serious trouble in reproducing accurate rate constants for hydrogen abstraction reactions due primarily to the less accurate predicted barrier heights. For reaction (1), the calculated B3LYP-TST rate constants were grossly in error compared to the experimental ones. The discrepancy factor is found to be at least 10 and could exceed 1000 for low temperatures (data not shown). The calculated BHHLYP-TST and (MP2//CASSCF)-TST rate constants for temperature range

Table 8
Calculated (MP2//CASSCF)-TST rate constants ($cm^3\ mol^{-1}\ s^{-1}$) compared to experimental values

$T(K)$	k_{TST}	$k_{TST/W}$	$k_{TST/ZCT}$	Exp.	DF
200	2.78(−20)	5.32(−19)	3.78(−15)		
250	1.51(−18)	1.90(−17)	5.56(−15)		
298	2.01(−17)	1.84(−16)	8.29(−15)	4.92(−15)	1.68
300	2.19(−17)	1.99(−16)	8.43(−15)	5.14(−15)	1.64
350	1.51(−16)	1.05(−15)	1.30(−14)	1.26(−14)	1.03
400	6.51(−16)	3.61(−15)	2.02(−14)	2.48(−14)	1.22
450	2.06(−15)	9.45(−15)	3.11(−14)	4.19(−14)	1.34
500	5.25(−15)	2.05(−14)	4.70(−14)	6.39(−14)	1.35
550	1.14(−14)	3.89(−14)	6.94(−14)	9.01(−14)	1.30
600	2.21(−14)	6.67(−14)	9.99(−14)	11.9(−14)	1.19
650	3.91(−14)	1.06(−13)	1.40(−13)	1.52(−13)	1.08
700	6.42(−14)	1.59(−13)	1.93(−13)	1.88(−13)	1.03
750	9.97(−14)	2.28(−13)	2.59(−13)	2.25(−13)	1.15
800	1.47(−13)	3.15(−13)	3.40(−13)	2.63(−13)	1.29
850	2.10(−13)	4.21(−13)	4.39(−13)	7.19(−13)	1.63
900	2.89(−13)	5.49(−13)	5.56(−13)	9.34(−13)	1.68
950	3.87(−13)	6.99(−13)	6.97(−13)	11.8(−13)	1.69
1000	5.07(−13)	8.74(−13)	8.60(−13)	14.5(−13)	1.68
1050	6.49(−13)	1.08(−12)	1.05(−12)	1.76(−12)	1.68
1100	8.16(−13)	1.31(−12)	1.26(−12)	2.09(−12)	1.66
1200	1.23(−12)	1.85(−12)	1.77(−12)	2.84(−12)	1.60
1300	1.77(−12)	2.53(−12)	2.41(−12)	3.67(−12)	1.52
1400	2.44(−12)	3.34(−12)	3.18(−12)	4.57(−12)	1.44
1500	3.25(−12)	4.30(−12)	4.10(−12)	5.54(−12)	1.35
2000	9.71(−12)	1.15(−11)	1.10(−11)	1.07(−11)	1.03

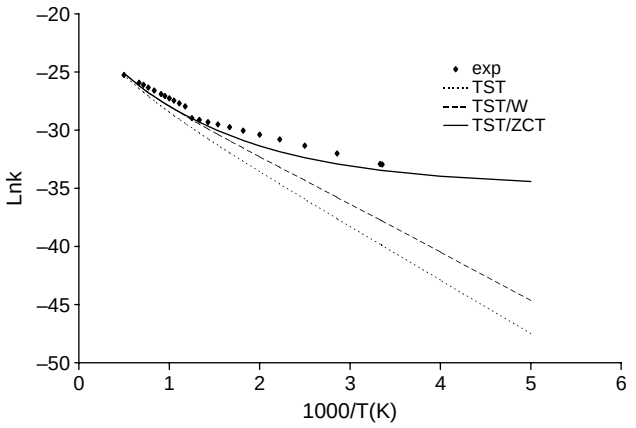

Fig. 3. Plot of logarithm of the BHHLYP-TST rate constants ($cm^3\ mol^{-1}\ s^{-1}$) versusb $1000/T(K)$.

from 200 to 2000 K are listed, respectively, in Tables 7 and 8 and compared to those measured by Baulch et al. for $300 \leq T \leq 800$ K and by Stang and Hampson for $800 < T \leq 2000$ K. The disagreement factors (DF) between the more accurately calculated and the experimental rate constants for all the considered temperatures were indicated. Figs. 3 and 4 show the logarithm plot of the calculated k_{TST}, $k_{TST/W}$ and $k_{TST/ZCT}$ rate constants and the measured ones versus $1000/T(K)$. It is worth noticing that from these k_{TST}, $k_{TST/W}$ and $k_{TST/ZCT}$ rate constants calculated by BHHLYP-TST method as a function of temperature, we could make similar observations to those found in the (MP2//CASSCF)-TST calculation: (i) the tunnel effect contribution to reaction (1) is assumed to be important even for ambient temperatures, (ii) the Wigner method accounts for only a part of the tunneling contribution and iii) among the calculated TST, TST/W and TST/ZCT rate constants, the most accurately predicted ones are those calculated using the later method. The disagreement factor between the calculated BHHLYP-TST/ZCT and (MP2//CASSCF)-TST/ZCT rate constants and the experimental ones never exceeded, respectively, 2.87 and 1.70 and could approaches the unity. This reasonable agreement confirms the reliability of the (MP2//CASSCF)-TST/ZCT method in predicting accurate thermal rate constants [19] and shows that the BHHLYP-TST method can be an adequate choice for kinetic study of reaction (1). Further tests on this method for other hydrogen abstraction reactions could be useful since DFT methods are less expensive than ab initio ones using the same basis set.

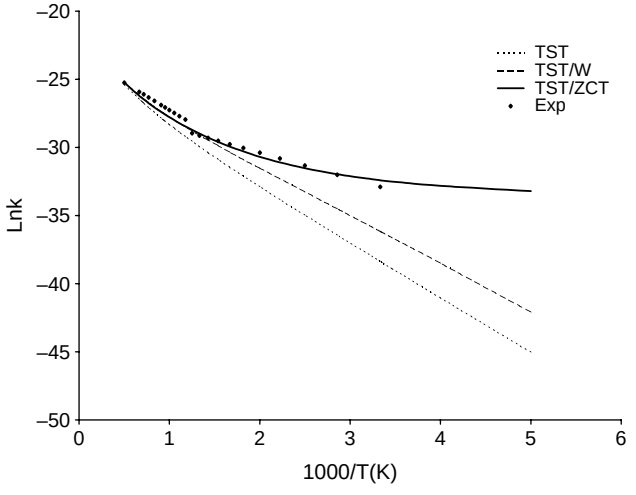

Fig. 4. Plot of logarithm of the (MP2//CASSCF)-TST rate constants ($cm^3\ mol^{-1}\ s^{-1}$) versus $1000/T(K)$.

4. Conclusion

We tested two DFT methods BHHLYP and B3LYP on predicting accurate kinetic parameters and rate constants of a hydrogen abstraction reaction involving O–H bond breaking. After adding ZPE and BSSE corrections, B3LYP calculation predicted, a value of 2.34 kcal mol^{-1} for the barrier height which was very low compared to the experimental ones fitted from Arrhenius expressions. The resulting rate constants were grossly in error. The well established trouble of the B3LYP method in predicting accurate rate constant for hydrogen abstraction reaction involving C–H bonds breaking was also observed for reaction (1) involving O–H bond breaking. The ZPE and BSSE corrected barrier height calculated using the BHHLYP method was found to be 9.31 kcal mol^{-1} which approaches the MP2//CASSCF value 8.08 kcal mol^{-1} and lays in the range of the experimental values (3.75–9.44 kcal mol^{-1}). The disagreement factor between the calculated (MP2//CASSCF)-TST and BHHLYP-TST/ZCT and the experimental rate constants never exceeded, respectively, 1.7 and 2.9 for all considered temperatures. This reasonable agreement confirms the reliability of the (MP2//CASSCF)-TST/ZCT method in predicting accurate thermal rate constants and suggests that DFT electronic structure calculation using the BHHLYP method can be one of the adequate choices to be used with the TST method in predicting accurate rate constants for hydrogen abstraction reactions.

Acknowledgements

The authors are grateful to Prof. Donald G. Truhlar, Department of Chemistry University of Minnesota, for the license access to POLYRATE 7.3.1 program.

We would like to thank Mr A. Hajji from the Engineering School of Sfax for his help with English.

References

[1] Angela Violi, Thanh N. Truong, Adel F. Sarofim, J. Phys. Chem. A 108 (2004) 4846.
[2] Shaowen Zhang, Thanh N. Truong, J. Phys. Chem. A 107 (2003) 1138.
[3] Thanh N. Truong, J. Chem. Phys. 113 (2000) 4957.
[4] Jing-Fa Xiao, Ze-Sheng Li, Yi-Hong Ding, Jing-Yao Liu, Xu-Ri Huang, Chia-Chung Sun, Phys. Chem. Chem. Phys. 3 (2001) 3955.
[5] Branko S. Jursic, J. Chem. Soc., Faraday Trans. 92 (1996) 3467.
[6] Kyu-Man Jeong, Frederick Kaufman, J. Phys. Chem. 86 (1982) 1816.
[7] Jaime M. Martell, Anil K. Mehta, Philip D. Pacey, Russell J. Boyd, J. Phys. Chem. 99 (1995) 8861.
[8] Sanja Sekusak, Klaus R. Liedl, Bernd M. Rode, Aleksander Sabljic, J. Phys. Chem. A 101 (1997) 4245.

[9] Andrea Bottoni, Gabriella Poggi, Salvator S. Emmi, J. Mol. Struct. (Theochem) 279 (1993) 299.
[10] Baoshan Wang, Hua Hou, Yueshu Gu, J. Chem. Phys. 112 (2000) 8458.
[11] Branko S. Jursic, Int. J. Quantum Chem. 65 (1997) 75.
[12] Joseph L. Durant, Chem. Phys. Lett. 256 (1996) 595.
[13] Sergei Skokov, Ralph A. Wheeler, Chem. Phys. Lett. 271 (1997) 251.
[14] Benjamin J. Lynch, Patton L. Fast, Maegan Harris, Donald G. Truhlar, J. Phys. Chem. A 104 (2000) 4812.
[15] Oksana Tishchenko, Eugene S. Kryachko, Minh Tho Nguyen, J. Mol. Struct. 615 (2002) 247.
[16] Annelies Delabie, Steven Creve, Betty Coussens, Minh Tho Nguyen, J. Chem. Soc., Perkin Trans. 2 (2000) 977.
[17] Joseph S. Francisco, S.P. Sander, Mol. Phys. 85 (1995) 1069.
[18] Y. Tarchouna, M. Bahri, N. Jaïdane, Z. Ben Lakdar, J.P. Flament, J. Chem. Phys. 118 (2003) 1189.
[19] Y. Tarchouna, M. Bahri, N. Jaïdane, Z. Ben Lakdar, J.P. Flament, J. Mol. Struct. 664–665 (2003) 189.
[20] M. Bahri, Y. Tarchouna, N. Jaïdane, Z. Ben Lakdar, J.P. Flament, J. Mol. Struct. 664–665 (2003) 229.
[21] Roberta G. Susnow, Anthony M. Dean, William H. Green Jr., Chem. Phys. Lett. 312 (1999) 262.
[22] D.L. Baulch, C.L. Cobos, R.A. Cox, C. Esser, P. Frank, Th. Just, J.A. Kerr, M.J. Pilling, J. Troe, R.W. Walker, J. Warnatz, J. Phys. Chem. Ref. Data 21 (3) (1992) 411.
[23] J. Warnatz, in: W.C. Gardiner (Ed.), Combustion Chemistry, Springer, New York, 1984.
[24] W. Tsang, R.F. Hampson, J. Phys. Chem. Ref. Data 15 (1986) 1087.
[25] M.W. Schmidt, K.K. Baldridge, J.A. Boatz, S.T. Elbert, M.S. Gordon, J.H. Jensen, S. Koseki, N. Matsunaga, K.A. Nguyen, S.J. Su, T.L. Windus, M. Dupuis, J.A. Montgomery, J. Comput. Chem. 14 (1993) 1347.
[26] T.H. Dunning Jr., J. Chem. Phys. 90 (1989) 1007.
[27] S.F. Boys, F. Bernardi, Mol. Phys. 19 (1970) 553.
[28] H. Nakano, J. Chem. Phys. 99 (1993) 7983.
[29] H. Nakano, Chem. Phys. Lett. 207 (1993) 372.
[30] Thanh N. Truong, Donald G. Truhlar, J. Chem. Phys. 93 (1990) 1761.
[31] E. Wigner, Z. Phys. Chem. B 19 (1932) 203.
[32] A. Gonzalez-Lafont, T.N. Truong, D.G. Truhlar, J. Chem. Phys. 95 (1991) 8875.
[33] R. Steckler, Y. -Y. Chuang, P.L. Fast, E.L. Coitino, J.C. Corchado, W. -P. Hu, Y. - P.Liu , G.C. Lynch, K.A. Nguyen, C.F. Jackels, M.Z. Gu, I. Rossi, S. Clayton, V.S. Mellissas, B.C. Garrett, A.D. Issacson, D.G. Truhlar, POLYRATE-version 7.3.1, University of Minnesotta, Minneapolis, (1997)
[34] K.P. Huber, G. Herzberg, Molecular spectra and molecular structure Constants of Diatomic Molecules, Van Nostrand Reinhold, New York, 1979.
[35] René Fourier, Andrew E. DePristo, J. Chem. Phys. 96 (1992) 1183.
[36] Vasiolios S. Melissas, D.G. Truhlar, J. Phys. Chem. 98 (1993) 875.
[37] M. Bahri, N. Jaïdane, Z. Ben Lakhdar, J.P. Flament, J. Chim. Phys. 96 (1999) 634.
[38] Kerwin D. Dobbs, David A. Dixon, Andrew Komornicki, J. Chem. Phys. 98 (1993) 8852.
[39] M.E. Jacox, Vibrational and Electronic Energy Levels of Polyatomic Transient Molecules, AIP, Woodbury, 1994.
[40] W.B. Olson, R.H. Hunt, B.W. Young, A.G. Maki, J.W. Brault, J. Mol. Spectrosc. 127 (1988) 12.
[41] C. Camy-Peyret, J.M. Flaud, J.W.C. Johns, M. Noel, J. Mol. Spectrosc. 155 (1992) 84.
[42] S. Klee, M. Winnewisser, A. Perrin, J.M. Flaud, J. Mol. Spectrosc. 195 (1999) 154.
[43] P.A. Giguere, T.K.K. Srinivasan, J. Raman Spectrosc. 2 (1974) 125.
[44] J.A. Boatz, M.S. Gordon, J. Chem. Phys. 93 (1989) 819.
[45] G. Schaftenaar, J.H. Noordik, Molden: a pre- and post-processing program for molecular and electronic structures, J. Comput. -Aided Mol. Des. 14 (2000) 123–134.
[46] R.B. Klemm, W.A. Payne, L.J. Stiff, Int. J. Chem. Kinet. 1 (1975) 61.
[47] Koussa H., Bahri M., Jaï N., dane, in preparation